Routing Protocol for Complex Three-dimensional Vehicular Ad Hoc Networks

Ying He[1], Xuelian Cai[1]*, Yankang Zhang[2], Xiaolei Han[1], Qin Lin[1], Changle Li[1]
[1]State Key Laboratory of Integrated Service Networks, Xidian University, Xi'an, Shaanxi, 710071 China
[2]Shengli Power Plant, Shengli Oilfield Company, SINOPEC, Dongying, Shandong, 257087 China
*xlcai@mail.xidian.edu.cn

***Abstract*—Due to the existence of three-dimensional (3D) scenarios in realistic Vehicular Ad hoc Network (VANET), such as the viaduct, tunnel and ramp, the distribution of vehicles is 3D. To the best of our knowledge, the issue of designing a routing protocol for 3D VANET has rarely been studied. Our previous work [10] has provided a Three-dimensional scenario oriented Routing (TDR) for the simple 3D scenario which contains two or more parallel roads with different heights. Because the distribution of nodes in the complex 3D scenarios has no rules and no obvious stratification phenomenon, TDR is not suitable for the complex 3D scenarios. Here the complex 3D scenarios are these flyover scenarios with many ramps and irregular arrangements in a large range. Therefore, we propose a novel routing protocol Complex Three-dimensional scenario oriented Routing (C-TDR) for the complex 3D scenarios. In C-TDR we introduce the concept of virtual neighbor and the completion process of neighbor list considering the feature of fluctuant transmission range of nodes in 3D VANET. Finally, we build a simulation scenario containing the simple 3D scene and the complex 3D scene and conduct the simulation for C-TDR. The C-TDR is shown to increase the packet delivery rate and decrease the end-to-end delay and hop count.**

Keywords—VANET; routing; complex 3D scenario

I. INTRODUCTION

Due to the existence of three-dimensional (3D) scenarios in realistic VANET, such as the viaduct, tunnel and ramp, it is a pressing matter to design a routing protocol for 3D VANET.

To the best of our knowledge, the issue of designing a routing protocol for 3D VANET has rarely been studied. The traditional existing routing protocols in VANET are mainly analyzed and designed based on ideal plane scenarios [1-6]. For example, VADD [7] is a protocol based on the idea of carrying and forwarding. In order to select the outgoing segment at intersection, VADD proposes a regional delay model. As the classic intersection-based geographic routing, GPCR [8] forwards packets to the special vehicles in the middle of the junctions, called coordinators, and then makes the important forwarding decision. CAR [9] selects a better path to transmit data packets through the route request and the discovery process. Our previous work has obtained some achievements about 3D VANET routing [10]. We can find that the routing protocol TDR which is proposed in our previous work is applied in the simple 3D scenarios, i.e. the scenarios of containing two or more parallel roads with different heights. To observe the characteristics of city road network, we can find that not only such simple 3D scenarios but also the complex 3D scenarios exist in realistic VANET environment. Here the complex 3D scenarios are these flyover scenarios with many ramps and irregular arrangements in a large area. Fig. 1 shows an example of the complex 3D scenario. Due to the intersection-based routing mechanism and the features of the complex 3D scenarios, the previous work TDR is not suitable for the complex 3D scenarios. Therefore, in this paper we propose a new routing protocol C-TDR for the complex 3D scenarios. The C-TDR mainly consists of 3D greedy forwarding strategy and 3D recovery strategy. The 3D greedy forwarding strategy is an extension method for planar greedy forwarding. The 3D recovery strategy contains projection strategy and improved FACE routing algorithm. Least square plane and more projection planes strategy are considered in projection strategy. The key content of the improved FACE routing is to present the improved Gabriel Graph (GG) extracted method based on the feature of fluctuant transmission range of nodes in 3D VANET. In addition, we introduce the concept of virtual neighbor and the completion process of neighbor list to avoid the problems that cased by the fluctuant transmission range of nodes in FACE routing. Finally, we conduct a simulation about the proposed routing protocol C-TDR. The simulation results show that C-TDR can increase the packet delivery rate and decrease the end-to-end delay and hop count in the realistic scenario containing the simple 3D scene and the complex 3D scene.

The rest of the paper is arranged as follows. The Section II presents the characteristics of 3D urban scenarios. Our proposed protocol C-TDR is illustrated in the Section III which is followed by simulation results and analyses. The last is the conclusion.

II. THE CHARACTERISTICS OF 3D URBAN SCENARIOS

To observe the characteristics of city road network, we can find that the urban area is divided into several blocks by freeway and backbone road. The characteristics of city road network in China are analyzed and summed up into the four basic forms in literature [11], namely grid road network, ring and radial road network, free road network and mixed type road network. From the above characteristics it is not difficult to conclude that the whole city area is still divided into several zones with the difference in the shape of zones, such as the

978-1-4799-6729-2/14/$31.00 ©2014 IEEE

DOI 10.1109/ICCVE.2014.133

Fig. 1. An actual complex three-dimensional interchange scenario

shape of zones in grid road network is rectangular, and the shape in free road network is irregular. Meanwhile other countries have come to the same conclusion [12].

From the above, we can conclude that 3D urban scenario is composed of several zones and the 3D feature is mainly reflect at the boundary or intersection of zones. In addition, we can also find that the road structure in zones is relatively simple, in which the main structure is a planar mesh and most 3D scenarios are simple that contain two or more parallel roads with different heights. While in the border or in the intersection of different zones, i.e. the free way or the backbone road, may appear some simple or complex overpass scenarios. So the routing protocols in 3D urban scenario can be divided into two parts. One part is the routing strategy in zones (including the boundary). Because of the possible existing of simple overpass scenarios in the border, the routing protocol TDR which is proposed in our previous work is suitable for the routing strategy in zones. The other part is the routing strategy in the intersection of different zones. There may be more complicated interchange scenarios which have much ramp and irregular arrangements and in which nodes distribution is without obvious stratification phenomenon and the distribution in 3D space is without rules. So TDR is not suitable for the complex 3D scenarios which are likely to appear in the intersection of different zones. From the above analyses, it is need to propose a routing protocol for complex 3D scenarios.

III. C-TDR PROTOCOL

Based on the above analysis, we put forward a novel protocol named C-TDR. The C-TDR is a geographic routing protocol and is mainly composed of two parts, respectively, 3D greedy forwarding strategy and 3D recovery strategy. The 3D greedy forwarding is a 3D extension method of planar greedy forwarding. The 3D recovery strategy is a solution for local maximum in 3D VANET.

A. 3D Greedy Forwarding Strategy

The fundamental principle of greedy forwarding is that a node forwards its packet to its neighbor that is closest to the destination. In the greedy forwarding strategy, one node is better than the sending node means the node is nearer to the destination than the sending node. This is the traditional greedy forwarding strategy used on the network in which the nodes distribution is planar. In the complex 3D urban scenarios of VANET, we also consider similar forwarding strategy, but all nodes' positions in the forwarding strategy are represented by 3D coordinates and the distance is calculated as

$$d = \sqrt{(x_1 - x_2)^2 + (y_1 - y_2)^2 + (z_1 - z_2)^2} \tag{1}$$

In Fig. 2, the node U refers to the sending node, the node T refers to the destination node of the current packet transmission, and V1, V2, V3 are the neighbor nodes of the node U. According to the 3D greedy forwarding, V3 will be chosen as the next hop.

B. 3D Recovery Strategy

3D recovery strategy consists of projection strategy and the improved FACE routing algorithm. Least square plane and more projection planes strategy are considered in projection strategy. The improved FACE routing algorithm takes into account the impact of volatility transmission range on a spanning sub-graph and introduces the concept of virtual neighbor and completion process of neighbor list to avoid the problem caused by volatility transmission distance.

1) Projection strategy: The projection strategy includes the following three parts: least squares projection, behavior values and multi-projection planes. Least squares projection means that we do not choose the projection plane arbitrarily but choose the plane with the minimum sum of the square of the distances between all nodes and their corresponding projection points. Behavior value refers to the index of the hop counts and the recalculated least squares projection plane. Hop counts is the number of neighbor hops which are projected to the projection plane. Presets the behavior value, if the packet cannot reach the destination node through a certain number that equals to the behavior value of hops, the node has to recalculate the projection plane. Multi-projection planes refer to that the projection plane in the recovery strategy is not invariable. We adopt multi-projection planes for avoiding routing loop and data loss caused by the use of FACE routing in a particular projection plane.

a) Least squares projection: When 3D greedy forwarding strategy fails, the local optimal node will start the 3D recovery strategy. At first, local optimal node needs to calculate the least squares projection plane. As we know, a plane can be expressed by its normal vector and a point in the plane, that means

$$\vec{n} \cdot (p - p_0) = 0 \tag{2}$$

or

$$a(x - x_0) + b(y - y_0) + c(z - z_0) = 0 \tag{3}$$

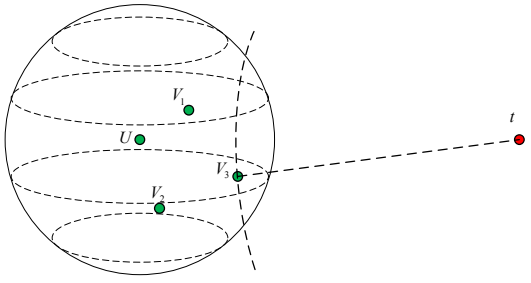

Fig. 2. The 3D greedy forwarding strategy

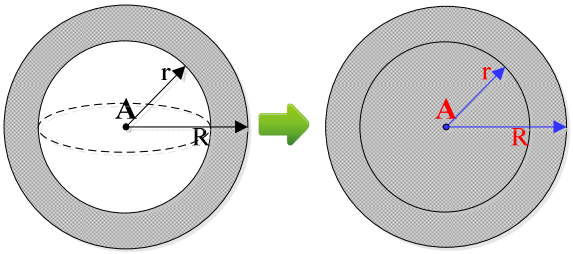

Fig. 3(a) fluctuant transmission range of A

Fig. 3(b) projected transmission range of A

Fig. 3. The example transmission range of node in 3D VANET

where $\vec{n}=(a,b,c)$ is the normal vector, $p_0=(x_0,y_0,z_0)$ is a random point in the plane. Assume the number of nodes that need to be projected is m, thus the least squares projection plane must contain the following nodes:

$$\left(\frac{1}{m}\sum_{i=1}^{m}x_i,\frac{1}{m}\sum_{i=1}^{m}y_i,\frac{1}{m}\sum_{i=1}^{m}z_i\right) \tag{4}$$

where (x_i,y_i,z_i) is the coordinate of the node i.

$$p_0=\left(\frac{1}{m}\sum_{i=1}^{m}x_i,\frac{1}{m}\sum_{i=1}^{m}y_i,\frac{1}{m}\sum_{i=1}^{m}z_i\right) \tag{5}$$

Let r_i be the Euclidean distance between the node i and the corresponding projection points, then the least square plane is the plane that has the minimal value of $\sum_{i=1}^{m}r_i^2$. The normal vector of the plane can be determined by using the singular value decomposition method. There is a problem about the number of the nodes that need to be projected, namely the value of m. If the value of m is small, it will case a significant amount of computation. Because it requires the subsequent forwarding nodes to calculate the least squares projection plane frequently. Conversely, if the value of m is high, the delivery rate cannot be guaranteed. We will use the improved FACE routing algorithm to transmit the data in the projection plane. If all the forwarding nodes are projected onto the plane, the node topology will be greatly distorted and the delivery rate cannot be guaranteed.

b) Behavior value: It refers to the number of nodes involved in each calculation of least squares projection plane, namely the m. If the hop count reaches the preset behavior value, but the data packet still does not reach the destination, the current node has to recalculate the projection plane. The calculation of each projection plane needs the coordinates of all neighbor nodes that located within m hops range of the current node. The mechanism makes the improved FACE routing algorithm on projection plane more robust and adaptive. It can avoid routing loop that caused by intersecting link by recalculating the projection plane.

*c) Multi-projection planes:*The projection plane in the recovery strategy is not only or invariable. If the hop count reaches the behavior value before the data reaches the destination, the current node will recalculate the projection plane.

2) Improved FACE routing algorithm: In wireless network, the forward area of node is called a routing hole when it transmits its packet to the node which is not nearer to the destination. Routing hole may lead to the failure of packet transmitting. When there exists routing hole, node should establish the node topology through monitoring the nodes around the hole and use right hand rule to bypass the routing hole to transmit packet. This method is called FACE routing.

a) The transmission range model: The transmission range of nodes in 3D VANET is fluctuating. A typical example is that maximum transmission distance in the same layer of nodes on the overpass is greater than that of nodes in the inter-layer direction. Because of the characteristics of the fluctuated transmission range, the corresponding 3D transmission range model is shown in Fig. 3(a). All nodes in the sphere with the radius of r can communicate directly with node A, all nodes out of the sphere with the radius of R cannot communicate directly with node A, some nodes within the shadow area can communicate directly with node A, but some cannot. Since our recovery strategy is carried out on the projection plane, we concern about the characteristics of transmission range in the projection plane. From the 3D transmission range model, we can get the transmission range model in the projection plane as shown in Fig. 3(b) easily. In Fig. 3(b), all nodes within the shadow, some of them can communicate directly with node A, but some cannot.

b) The principle of extracting GG sub-graph: The link between node u and node v is retained in the extracted GG sub-graph if and only if there are no other nodes within the round with the diameter of edge $\overline{uv}$. In 3D VANET, because of the characteristic of fluctuating transmission range we may encounter the following problem. In Fig. 4, node u can directly communicate with node v, that means $v\in L(u)$ and $u\in L(v)$ where $L(u)$ and $L(v)$ represent the neighbor list of node u and node v, respectively. When node u determines whether the link between node u and node v is retained in the extracted GG sub-graph, node u will delete the link between node u and node v, because node w is in the round with the diameter of edge $\overline{uv}$ and $w\in L(u)$. However, when node v determines whether the link between node u and node v is retained in the extracted GG sub-graph, node v may retained

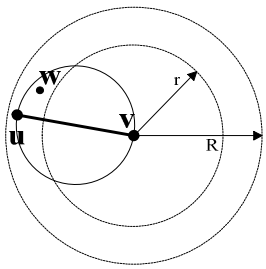

Fig. 4. The analysis-aided graph

```
1.neighbor list completion process (){
2.traverse all nodes in L(v){
3.      while (u belongs to L(v)){
4.              while (w belongs to L(u)){
5.                      if (w belongs to D_uv){
6.                              node u sends the packet "(new neighbor, w)" to v;
7.                              node u transmits another packet "(new neighbor, v)" to w;
8.                      }
9.              }
10.     }
11.     while (u belongs to L(v)){
12.             while (w belongs to L(u)){
13.                     if (node v receives the packet "(new neighbor, w)"){
14.                             if (node w is in the neighbor list of node v)
15.                                     v discards the packet;
16.                             else
17.                                     v adds w to its neighbor list L(v) ;
18.                     }
19.             }
20.     }
21.}
22.add nodes in L(v) that have been treated through the above process to L`(v) ;
23.while (nodes in L(v) and L`(v) are the same&& no new packet is received)
24.     the neighbor list completion process of node v ends;
25.}
```

Fig. 5. The pseudo-code of the neighbor list completion process

the edge $\overline{uv}$, since node v may not find the existence of node w, namely $w \notin L(v)$. From the above discussion, we can conclude that in 3D VANET, the extracted GG sub-graph is not unique. The problem unlikely occurs in planar scenarios in which the transmission ranges of all nodes are considered to be the same. Therefore, our improved FACE routing algorithm proposes a neighbor list completion process for each node before generating GG sub-graph, which aims to solve this problem and is the biggest difference between the improved FACE routing and the original FACE routing.

c) The neighbor list completion process: First, we introduce the concept of the virtual neighbor that aims to avoid the problem discussed in generating GG sub-graph. Take node A in Fig. 3(b) as an example. The virtual neighbors of node A refer to nodes which locate in the shadow area and cannot communicate directly with node A but can communicate with it via multi-hop communication. Then we introduce a completion process of neighbor list and the method to join the virtual neighbors. Assume that we need to complete the neighbor list of node v. In the following procedure, $D_{u,v}$ represents all nodes that locate within the circle with the diameter of edge $\overline{uv}$. $L(u)$ and $L(v)$ refer to the neighbor list of node u and node v, respectively. $\forall u \in L(v)$, check each node $w \in L(u)$, if $w \in D_{u,v}$, then the node u sends the packet "(new neighbor, w)" to v, and transmits another packet "(new neighbor, v)" to w. The data packet also contains the location information of the new neighbor. Add nodes in $L(v)$ that have been treated through the above process to the set $L'(v)$. When the node v receives a packet "(new neighbor, w)", it will check whether the node w has been a neighbor in its neighbor list. If it is, the packet is discarded. If it is not, v will add w to its neighbor list $L(v)$ with the path from node w to node v, and w is a virtual neighbor of v. The virtual neighbors added to $L(v)$

```
1.when (a node receives a data packet){
2.      select the next hop based on the 3D greedy forwarding strategy;
3.      if (3D greedy forwarding strategy fails)
4.              switch the 3D greedy forwarding to 3D recovery strategy();
6.      else
7.              forward the data packet to the next hop;
8.}
9.3D recovery strategy(){
10.     preset the behavior value m;
11.     calculate the least squares projection plane;
12.     complete its neighbor list based on the neighbor list completion process();
13.     extract the GG sub-graph;
14.     select the next hop based on right-hand principle on the GG sub-graph;
15.     forward the data packet to the next hop;
16.     if (the subsequent forwarding node receive the packet){
17.             if (it is closer to the destination than the packet entered in the 3D
18.             recovery strategy)
19.                     switch the forwarding mode to 3D greedy forwarding;
20.             else{
21.                     if (the data packet has been transmitted through m hops
22.                     from the packet entered in the 3D recovery strategy){
23.                             if (the current node is the destination)
24.                                     forwarding process ends;
25.                             else
26.                                     recalculate the projection plane;
27.                     }
28.                     else
29.                             forward the packet to the next hop;
30.             }
31.     }
32.}
```

Fig. 6. The pseudo-code of the C-TDR

also need to be treated as the above process. When $L'(v) = L(v)$ and no new packet is received, the neighbor list completion process of v ends, and the obtained $L(v)$ at this time is the complete neighbor list. Fig. 5 is the pseudo-code of the process. Not only the actual neighbors and the virtual neighbors, but the paths from node v to the virtual neighbors are also stored in the complete neighbor list. After all neighbor nodes on the projection plane finish the completion process, we start to extract GG sub-graph. Fig. 6 is the pseudo-code of the C-TDR.

IV. Simulation Results and Analysis

In this section, we study the performance of C-TDR via Network Simulator version 2.34 (NS-2) [13]. We modelled the 3D scenario in NS-2 by extending the scenario coordinates. We successfully add the z-axis coordinate for each node through modifying some files, such as ns2.34/common/mobile.cc, ns2.34/Topology.pm, etc. We evaluate the performance of C-TDR with the TDR and 3D-GPSR. The C-TDR is an extension of our previous work TDR [10], so we choose TDR as one of the contrast protocols. GPSR is the most fundamental and classic geographic routing protocol in VANETs. Since the existing routing protocols rarely consider 3D scenario in VANETs and we take GPSR as the research object to analyze the issues in our previous work [10], we take 3D-GPSR as another contrast protocol.

A. Simulation Settings

The simulation scenario parameters are shown in Table 1. We set the simulation scenario as shown in Fig. 7, a grid

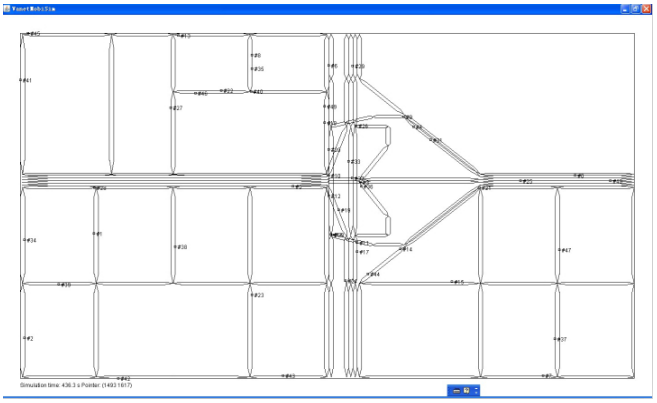

Fig. 7. The simulation scenario

region of 2100m*2100m*20m, urban environment. The center of the scenario is a complex overpass of four layers which reflects a complex 3D scenario. There are several parallel layered 3D scenarios described by straight roads of nonzero coordinates on z axis on roads that connected with this complex overpass. There are 40-190 vehicles randomly distributed on the roads at the beginning of the simulation. Each vehicle's velocity ranges from 30km/h to 60km/h. The map and node track files are generated by the vehicular mobility model generator VanetMobiSim [14]. The simulation time is 500s and each simulation running contains 10 random source-destination pairs. The mobility model in this scenario we used is Intelligent Driver Model (IDM) [15]. The mobile model makes the motion state of each vehicle in the scene such as velocity, acceleration by the surrounding vehicles' restrictions to keep a safe distance. We repeat the simulation process 20 times for a given scenario.

B. Results and Analysis

Fig. 8 illustrates the variation of average hop count with the increase of the number of nodes. From the chart we can see that the average hop count generally shows a decreasing trend along with the increase of the number of nodes. When the number of nodes is more than 140, with the continuous increase of the number of nodes, the average hop count gradually stabilizes. Because the probability of the local maximum is smaller with the increase of nodes, so the packet does not need to sacrifice hops for guaranteed delivery and also is along the direction to the destination. In addition, the number of neighbor nodes increases along with the increase of the number of nodes, that is the probability that the packet is transmitted farther can be high. However, with the continuous increasing of the number of nodes, the advantage in term of average hop count brought by the above reasons is no more obvious. Therefore, the average hop count does not continue reducing but gradually stabilized. Relative to TDR and 3D-GPSR, the combination routing protocol can obtain the less hop count. This is because in the TDR protocol, the complex 3D scenario part leads to more selection process of the intersection-destination, which will inevitably produce hop unnecessarily. In 3D-GPSR, although the 3D distribution can be identified, only the greedy forwarding principle cannot avoid frequent inter-layer transmission so that the packet delivery generates hop unnecessarily. In C-TDR, it can not only identify the 3D nodes distribution, but also have a design

TABLE I. SIMULATION SCENARIO PARAMETERS

Simulation area	2100m*2100m*20m
Number of vehicles	40-190
Simulation time	500 sec
Intra-layer transmission range	250m
Inter-layer transmission range	200m
Traffic model	10 cbr
CBR interval	0.5s
Data packet size	512 bytes
Beacon interval	1s
The propagation model	Two Ray Ground
MAC layer	IEEE 802.11 DCF
Channel rate	2Mbps

to avoid the selection process of the intersection-destination. So the routing hops will be relatively less.

Fig. 9 depicts the results of the packet delivery ratio varying with the increase of the number of nodes. From this figure, we can see that the packet delivery rate of these three protocols appear first upward and then downward trend with the increase of the number of nodes. When there are a small number of nodes, these three protocols may suffer from frequently links break, so the delivery rates are low. With more nodes, the network condition becomes favorable and the link becomes stable, moreover, the probability of the local maximum is smaller, so the delivery rate appears upward trend. However, with the continuous increase of the number of nodes, the interference could increase and damage the traffic delivery, so the curve appears a download trend. The average packet delivery rate of the C-TDR is higher than that of TDR and 3D-GPSR. This is mainly because the improved FACE routing of C-TDR is to ensure the packet delivery ratio. However, TDR and 3D-GPSR protocols have no extra mechanism to ensure the packet delivery ratio. In general, the packet delivery ratio

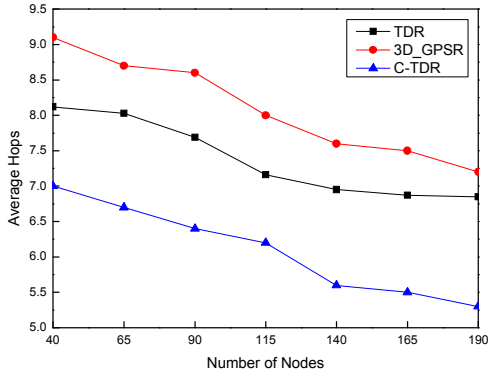

Fig. 8. Average hops vs number of nodes

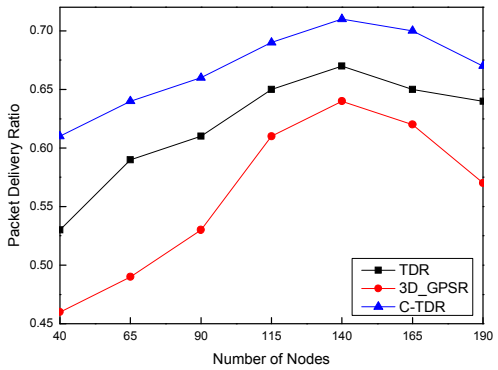

Fig. 9. Packet delivery ratio vs number of nodes

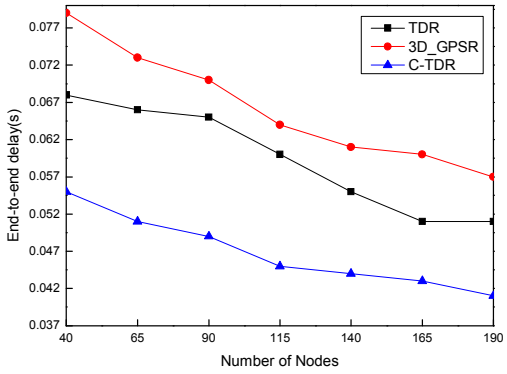

Fig. 10. End-to-end delay vs number of nodes

of C-TDR is 7.83% higher than TDR and 19.2% higher than 3D-GPSR.

As shown in Fig. 10, we compare the performance of three protocols in term of the average end-to-end delay. As we can see, the end-to-end delay decreases along with the increase of the number of nodes. When there are sufficient nodes in the network, with the continuous increase of the number of nodes, the end to end delay is reduced by a small margin, which is in line with the above simulation result about hop count. C-TDR can get the shortest end to end delay which is mainly because the protocol routing hops decrease. This advantage is more obvious when the node density is relatively large, and the delay of C-TDR is 21.2% lower than TDR and 29.3% lower than 3D-GPSR.

V. Conclusion

The issue of designing a routing protocol for 3D VANET is urgent to be solved. The routing protocol TDR that our previous work has presented is designed for the simple 3D scenarios. Depending on the analysis of the characteristics of 3D urban scenarios, we find that TDR is not suitable for the complex 3D scenarios. Therefore, we propose a new routing protocol C-TDR for the complex 3D scenarios. C-TDR uses improved FACE routing algorithm on the least squares projection plane in order to ensure the delivery rate of 3D VANET. And the key content of C-TDR is to present an improved method to extract the GG sub-graph based on the feature of fluctuant transmission range of nodes in 3D VANET. Because the improved FACE routing algorithm takes into account the 3D distribution of nodes and the characteristics of fluctuant transmission range of nodes in 3D VANET, C-TDR is more fitting the realistic scenario and ensures the overall routing performance. The simulation results also reflect that the C-TDR can achieve higher packet delivery rate, fewer hop count and lower end-to-end delay compared with the other two protocols. The delay of C-TDR is 21.2% lower than TDR and 29.3% lower than 3D-GPSR. The packet delivery ratio of C-TDR is 7.83% higher than TDR and 19.2% higher than 3D-GPSR.

Acknowledgment

This work was supported by the National Natural Science Foundation of China under Grant No. 61271176 and No. 61401334, the National Science and Technology Major Project under Grant No. 2013ZX03004007-003, the Fundamental Research Funds for the Central Universities, and the 111 Project (B08038).

References

[1] B. Karp, H. T. Kung. GPSR: Greedy Perimeter Stateless Routing for Wireless Networks. Mobile Computing and Networking, 2000. 243-254.

[2] C. Lochert, M. Mauve, H. Füßler, et al. Geographic Routing in City Scenarios. ACM SIGMOBILE Mobile Computing and Communications Review, 2005, 9(1): 69-72.

[3] B. C. Seet, G. Liu, B. S. Lee, et al. A-STAR: A Mobile Ad Hoc Routing Strategy for Metropolis Vehicular Communications. Mobile and Wireless Communications, 2004, 3042: 989-999.

[4] J. Zhao, G. Cao. VADD: Vehicle-Assisted Data Delivery in Vehicular Ad Hoc Networks. IEEE Transactions on Vehicular Technology, 2008, 57(3): 1910-1922.

[5] M. Jerbi, S. M. Senouci, R. Meraihi, et al. An Improved Vehicular Ad Hoc Routing Protocol for City Environments. IEEE International Conference on Communications, 2007. 3972-3979.

[6] M. Jerbi, S. M. Senouci, et al. GyTAR: Improved Greedy Traffic Aware Routing protocol for Vehicular Ad hoc Networks in City Environments. ACM International Workshop on Vehicular Ad Hoc Networks, 2006, 2006: 88–89.

[7] J. Zhao, G. Cao. VADD: Vehicle-Assisted Data Delivery in Vehicular Ad Hoc Networks. IEEE Transactions on Vehicular Technology, 2008, 57(3): 1910-1922.

[8] C. Lochert, M. Mauve, H. Füßler, et al. Geographic Routing in City Scenarios. SIGMOBILE Mobile Computing and Communications Review, 2005, 9(1): 69-72.

[9] V. Naumov, T. R. Gross. Connectivity-Aware Routing (CAR) in Vehicular Ad-hoc Networks. 26th IEEE International Conference on Computer Communications (INFOCOM 2007), 2007. 1919-1927.

[10] Q. Lin, C. Li, X. Wang, L. Zhu. A Three-dimensional Scenario Oriented Routing Protocol in Vehicular Ad Hoc Networks. IEEE Vehicular Technology Conference (VTC2013-Spring), Dresden, Germany, 2013.

[11] J. Duan, J. Li. The Structure Characteristic Research of Urban Traffic Network Based on Spatial Analysis. Acta Scientiarum Naturalium Universitatis Sunyatseni, 2002, 41(6): 105-108.

[12] X. Shi, J. Yu. Traffic Characteristics of Medium City in Fast Urbanization Area. Journal of Traffic and Transportation Engineering, 2010, 10(2): 88-94.

[13] The network simulator ns-2, http://www.isi.edu/nsnam/ns.

[14] J. H. aerri, F. Filali, C. Bonnet, M. Fiore. VanetMobiSim: Generating Realistic Mobility Patterns for VANETs. In ACM 3rd International Workshop on Vehicular ad hoc Networks, 2006. 96-97.

[15] A. Gainaru, C. Dobre, V. Cristea. A Realistic Mobility Model Based on Social Networks for the Simulation of VANETs. Vehicular Technology Conference (VTC2009-Spring), 2009.